AIAA SciTech Forum
January 3-7, 2022, San Diego, CA & Virtual
AIAA SCITECH 2022 Forum

10.2514/6.2022-2124

Multiscale Modeling of Streamers: High-Fidelity Versus Computationally-Efficient Methods

Lee R. Strobel*, Ngoc Cuong Nguyen† and Carmen Guerra-Garcia‡
Massachusetts Institute of Technology, Cambridge, MA, 02139, USA

A 2D axisymmetric streamer model is presented, using the fluid drift-diffusion approximation and the Hyridizable Discontinuous Galerkin (HDG) numerical method for spatial discretization. Numerical verification of the newly developed code is performed against the literature, demonstrating very good agreement with state-of-the-art codes, and results are presented for single-filament streamers using a plate-to-plate geometry, both with and without photoionization. Full-physics numerical models, such as the one presented, are computationally costly and not prone to parametrically studying streamers. Reduced order models of streamers are of interest to quantitatively relate streamer macroscopic parameters, but they need to be compared to higher-fidelity models to demonstrate their validity. In this contribution, the macroscopic parameter streamer model recently developed by our group is validated against the higher-fidelity model. The macroscopic parameter streamer model is based on the results of a reduced-order 1.5D quasi-steady model (i.e., 1D solution of the species continuity equations, 2D solution of Poisson equation, solved in the reference frame of the streamer). The comparison shows that the general trends captured by the macroscopic model, in terms of radius, speed, tip electric field and channel electric field relations, are in agreement with the results of the higher-fidelity simulations and limitations of the predictions are discussed.

I. Introduction

Streamers are transient electrical discharges that propagate as thin filament-like weakly conducting structures with very steep ionization fronts. The general appearance is that of a thin ionization region, the streamer head, with a very strong self-induced electric field that, if fed with seed electrons provides the driving mechanism of growth. Behind the streamer head an ionized channel is formed, the streamer body, which is quasi-neutral. Streamers find uses in a variety of applications, including industrial gas processing [1], biomedical [2] and plasma-assisted combustion [3]. They are also ubiquitous in atmospheric electricity phenomena, and are present in transient luminous events (such as sprites or blue jets [4] [5]) as well as during the initiation and propagation phases of leaders and lightning arcs [6].

Numerical models of streamers are useful to explore and predict the behavior of streamers in a variety of settings, from applications to natural events. Much development has been done in this area; however, simulating streamers numerically has proven to be highly challenging, due to the wide-range of length and time scales involved. Even in the case of a single filament, several time and length scales need to be resolved. Considering atmospheric pressure air conditions, the steep gradients in electric field and charged particle density present near the streamer tip are on the order of micrometers. The radius of a streamer filament is typically on the order of 0.1-1 mm; however, the length scales relevant to applications are typically tens or hundreds of millimeters. Considering time scales, the time scale for streamer propagation is on the order of nanoseconds; however, the timescales relevant for applications can be on the order of milliseconds, so the evolution of the streamer after it bridges the electrode gap, and its transition to a new discharge regime, would need to be tracked. Therefore, in order to accurately capture the physics relevant for streamers, a fluid model must use a very fine mesh to capture the steep gradients, but it must cover a large domain to consider application-relevant geometry. Since a small cell size is required, stability constraints generally require the use of very small time steps (often picosecond), which means that solving a streamer case for application-relevant timescales will necessitate solving a large mesh for potentially many millions of time steps. Several 2D and 3D fluid streamer models have been developed [7] [8] [9], which have been successful at analyzing streamers over short timescales; however, these models are typically computationally costly and do not allow the parametric exploration of the streamer operating

*Research Assistant, Aeronautics and Astronautics, lstrobel@mit.edu
†Principal Research Scientist, Aeronautics and Astronautics, cuongng@mit.edu, AIAA Member
‡Assistant Professor, Aeronautics and Astronautics, guerrac@mit.edu, AIAA Senior Member

envelope, which can be relevant to make the jump to models that can capture many-streamer interactions [10] or follow long streamer propagation in time.

One such reduced-order streamer model has been recently developed by our research group and is described in [11]. The model considers a 1.5D quasi-steady streamer: this uses a 1D model for the charged particle continuity equations and a 2D model for the electric field. The system of equations is solved in a quasi-steady approximation in the reference frame of the streamer and the streamer speed is found as an eigen value of the problem. This reduced order model was further explored by Pavan et al. to derive a Macroscopic Parameter Model (MPM), which describes the instantaneous (quasi-steady) state of a streamer through four, inter-related, key macroscopic parameters: speed, radius, tip electric field and channel electric field (note that this is different to the background electric field). If two of these parameters are known, then the instantaneous state of the streamer is completely defined. The relationship between these four parameters was also shown graphically, in the form of a macroscopic parameter model map (see Fig. 11 in [11]).

In this contribution, we present a newly-developed 2D axisymmetric fluid streamer model, which uses the Hybridizable Discontinuous Galerkin method in the discretization of the numerical equations. The paper first presents a detailed verification of the code against the literature. Then, it is used to quantify the accuracy of the MPM model of [11]. Future work will make use of this high-fidelity tool to address other outstanding challenges in streamer physics.

II. Physical Model

Physically, the streamer is modeled using equations that have become somewhat standard for the field. The evolution of the charged particle densities is modeled by the drift-diffusion equation (1):

$$\frac{\partial n_j}{\partial t} + \nabla \cdot (n_j \mathbf{v_j} - D_j \nabla n_j) = \dot{S}_{j,coll} + \dot{S}_{j,ph} \tag{1}$$

where n_j are the densities and D_j the diffusivities of each of the charged particle species. $\mathbf{v_j}$ is the drift velocity field for each species, calculated using equation (2):

$$\mathbf{v_j} = \mu_j \mathbf{E} \tag{2}$$

where here μ_j represents the mobility of each species and $\mathbf{E}$ is the electric field. $\dot{S}_{j,coll}$ is the net source term for each charged particle species due to collisional processes, mainly electron-impact ionization and attachment, given by equation (3):

$$\dot{S}_{j,coll} = n_j |\mathbf{v_j}| (\alpha_j - \beta_j) \tag{3}$$

where α_j and β_j are the ionization and attachment coefficients for each species, respectively. D_j, μ_j, α_j and β_j were all modeled analytically based on the output of the Boltzmann solver, Bolsig+ [12], using the local field approximation (i.e. that the aforementioned parameters are functions of the local electric field). The simulations consider air at atmospheric pressure conditions. Scattering cross-sections from the Phelps database [13] [14] were used for the O_2-electron impact reactions and cross-sections from the Siglo database [15] [16] were used for the N_2-electron impact reactions. Two charged particle species are considered in the model: electrons (n_e) and positive ions (n_i).

The electric field is governed by Poisson's equation for electrostatics (4):

$$\nabla \cdot (\nabla \phi) = -\frac{\rho}{\epsilon_0} \tag{4}$$

where ϕ is the electric potential ($\mathbf{E} = -\nabla\phi$) and ρ is the net space charge density, given by (5):

$$\rho = e(n_i - n_e) \tag{5}$$

$\dot{S}_{j,ph}$ is the source term due to photoionization. This is given by the integral equation below, proposed by [17]:

$$\dot{S}_{ph}(\mathbf{r}) = \int \frac{I(\mathbf{r}') f(|\mathbf{r} - \mathbf{r}'|)}{4\pi |\mathbf{r} - \mathbf{r}'|^2} d^3 r' \tag{6}$$

where $\mathbf{r}$ is the position where the ionization is being calculated, $\mathbf{r}'$ is the position where the photons are being generated, $I(\mathbf{r}')$ is the intensity of the generated photons and $f(|\mathbf{r} - \mathbf{r}'|)$ is an absorption function of the relative position. The integral has to be evaluated over the domain where ionizing photons are being generated. In this work we have

used the two-term parameterization proposed by Bourdon et al. [18], which results in the following set of Helmholz differential equations:

$$\nabla^2 \dot{S}^j_{ph}(\mathbf{r}) - (\lambda_j p_{O_2})^2 \dot{S}^j_{ph}(\mathbf{r}) = -A_j p^2_{O_2} I(\mathbf{r}) \tag{7}$$

$$\dot{S}_{ph}(\mathbf{r}) = \sum_j \dot{S}^j_{ph}(\mathbf{r}) \tag{8}$$

The advantage of this approximation is that, rather than solving an integro-differential problem, photoionization can be included by adding an additional set of partial differential equations to the system.Two sets of equation (7) need to be solved (one for each set of Bourdon parameters) and the solutions of those are then summed to give the total photoionization source term $\dot{S}_{ph}(\mathbf{r})$ (equation (8)).

III. Numerical Model

This work focuses on 2D axisymmetric simulations that were performed to solve the equations provided in section II. All of the fluid equations being solved (1, 4 and 7) were spatially discretized using the Hybridizable Discontinuous Galerkin (HDG) method, which is described in detail in [19]. The HGD method is similar to the finite element method; however, it allows for discontinuous solutions, which may be more suitable for modeling quickly-evolving physical phenomena that resemble discontinuities (such as compressible shocks, and possibly the steep ionization fronts of streamers). It can also be easily adapted to use higher-order elements, which can help to resolve the very steep gradients that are required for streamer simulations without greatly increasing cell count. It is also highly parallelizable; which is another trait that makes it a good choice for modeling streamers. The second-order backward differentiation formula (BDF2) implicit time stepping scheme was used with a fixed time step size of 0.7 ps.

An unstructured mesh with triangular cells was used. 3rd-order cells were used initially; however, the order was increased to 5th (to improve spatial resolution) for the cases with photoionization, after numerical oscillations were observed in the solution. Adaptive mesh refinement (AMR) was also employed, to ensure the regions with the steepest gradients were adequately resolved. The AMR scheme was based on the gradients present in the model, with the goal of limiting the maximum change in the tracked field variables across each cell. The AMR algorithm was run every 3 time steps and, for the cases presented in this paper, the cells were flagged for refinement if any of the following set of conditions were met: $\Delta E > 23.2$ kV/cm, Δn_e or $\Delta n_i > 4 \cdot 10^{19}$ m^{-3} or $\Delta(n_i - n_e) > 2 \cdot 10^{18}$ m^{-3}. Cells that were previously refined were flagged to be unrefined if all of the following set of conditions were met: $\Delta E < 11.6$ kV/cm, Δn_e and $\Delta n_i < 2 \cdot 10^{19}$ m^{-3} and $\Delta(n_i - n_e) < 1.2 \cdot 10^{18}$ m^{-3}. A minimum cell size of 2.5 μm was also set.

For the computational domain, a 2D plate-to-plate geometry was modeled using a rectangular domain, with the left-hand boundary representing the axis of symmetry of the streamer and the top/bottom boundaries representing the upper and lower electrode plates, across which a potential difference is applied. For the first case that was considered (without photoionization), a gap size between the plates of 25 mm was used. For subsequent cases that included photoionization, a gap size of 50 mm was used (to allow the streamer more space to run).

Regarding boundary conditions, for the Poisson equation (4), constant potentials were applied to the top and bottom boundaries. This was done to achieve a specific uniform background electric field in the domain - cases are presented with background fields of 15, 17.5, 20 and 23 kV/cm. Homogeneous Neumann boundary conditions were applied to the symmetry axis and right-hand boundary. For the electron density (n_e, equation 1), homogeneous Neumann conditions were applied to the symmetry axis and right-hand boundary. A Dirichlet condition equal to the background density was applied to the lower plate and an outflow condition was applied to the upper plate. For the positive ion density (n_i, equation 1), outflow conditions were applied to the lower plate and right-hand boundary; homogeneous Neumann was applied to the axis of symmetry and a zero Dirichlet condition was applied to the upper plate. For the Helmholtz equations for photoionization (equation (7)), zero Dirichlet conditions were applied to the lower plate and right-hand boundary and zero Neumann conditions were applied to the upper plate and axis of symmetry.

A uniform quasi-neutral background density (both electrons and ions) was applied to the simulations, using the same values as in [20]. For the initial case without photoionization, a background density of 10^{13} m^{-3} was used. For the subsequent cases that included photoionization, a background density of 10^9 m^{-3} was used.

A gaussian seed of positive ions was used as an initial condition to enhance the electric field and initiate the streamer. This is again very similar to the method used in [20], with the seed given by the following formula:

$$n_i(r,z) = N_0 \exp\left[-\frac{r^2 + (z - z_0)^2}{\sigma^2}\right] \tag{9}$$

where $N_0 = 5 \times 10^{18}$ m^{-3}, $\sigma = 0.4$ mm and z_0 is chosen such that the center of the seed is located 2.5 mm below the upper plate for run without photoionization and 3 mm below the upper plate for the subsequent runs.

IV. Numerical Verification of the Code

The HDG streamer code presented here has been verified against [20] and the results compare closely with the test cases that are presented there. Fig. 1a shows the adjusted streamer length versus time, with the results of the MIT HDG code plotted in red and results from the codes in [20] plotted black. Fig. 1b shows a comparison of the maximum electric field versus streamer length for the same codes. These are for the third test case in [20], which includes photoionization.

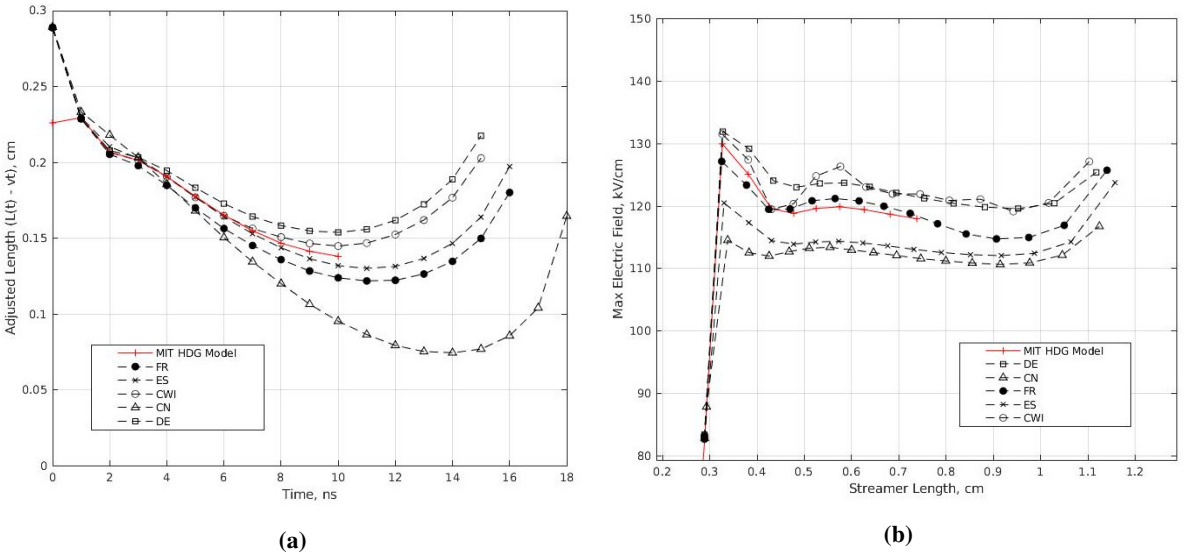

(a) **(b)**

Fig. 1 Comparison of results of 2D axisymmetric MIT HDG streamer model with results from [20], showing excellent agreement.

V. Results

One of the initial goals of this work was to compare the results of the 2D HDG model with the predictions of the macroscopic parameter model (MPM) map (briefly discussed in Section I and described in more detail in [11]). The macroscopic parameter model is based on the results of a quasi-steady, 1.5D, reduced-order model: whose main approximations are to calculate the particle densities in a 1D approximation (averaged across the cross-section of the streamer) as well as a quasi-steady solution (the streamer speed was calculated as an eigen value of the problem for the steady state solution in the reference frame of the head). In this paper we compare the results from that simplified model to the results using a transient 2D fluid streamer model, to investigate the validity of the assumptions that are being made in the MPM approximation, as well as the validity of the predictions when evaluating the transient propagation of streamers through the quasi-steady instantaneous approximation.

One of the challenges encountered when conducting this investigation was the prompt triggering of branching of the streamers, in a variety of tests considered. In particular, we used the HDG code to model both plate-to-plate and tip-to-plate electrode geometries, with a range of conditions and applied voltages, and in many cases, the streamer had a tendency to branch very soon after initiation. Several tip-to-plate geometries were tried, such as hyperbolic anodes similar to those described in [21]. A common issue was a lack of stability on the boundary of the tipped anode, where in small patches the electron density would go negative and then cause the solution to 'blow up'. The cause of this issue

seemed to be the use of too high a cell order. Reducing the cells from 7th to 3rd order made the solution more stable; however, issues were still encountered with streamers branching very soon after initiation. In the case of plate-to-plate geometries, fewer issues were encountered with numerical stability, likely due to the absence of the very high electric field gradients that are found in the vicinity of a sharp, tipped electrode. Suppression of branching structures was easier to achieve for cases with higher background electric fields. This is consistent with the findings of [22], which reported that single-filament streamers are more difficult to achieve below a threshold electric field of 14 kV/cm. Therefore, results will be presented here for single-filament streamers with a plate-to-plate geometry at electric fields of 15 kV/cm and above and we will focus on comparing those results to the macroscopic parameter model of [11].

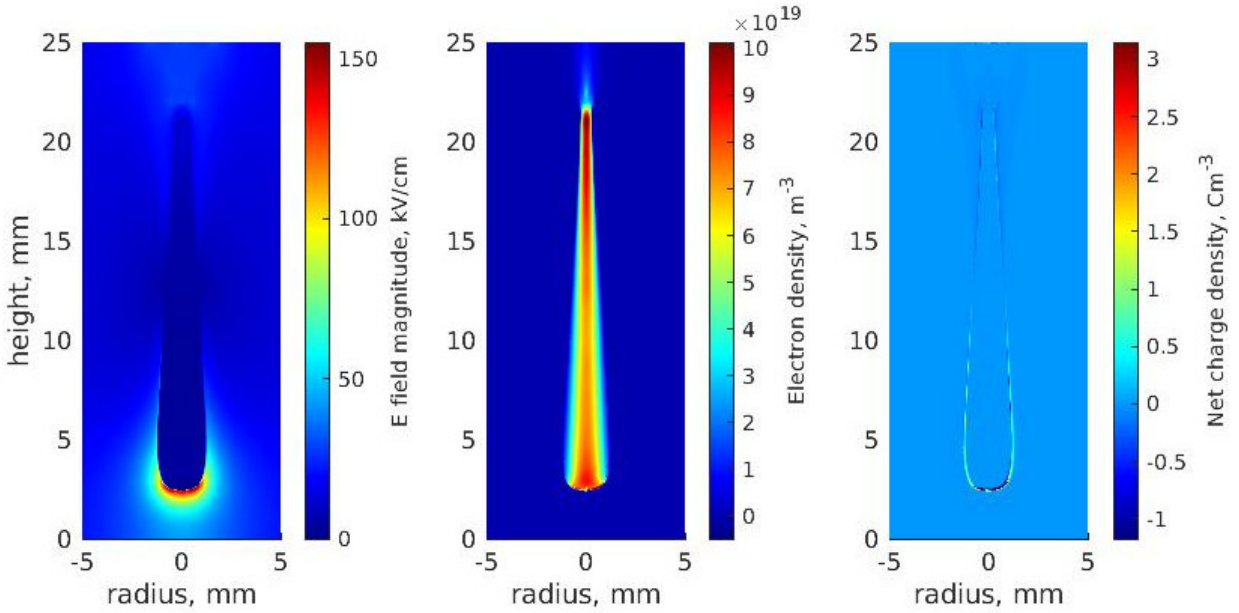

Fig. 2 Sample plots of electric field magnitude, electron density and net charge density for a positive streamer propagating in a background electric field. Simulations run substituting the photoionization model by a background density (time = 29 ns).

Figure 2 shows result plots of electric field magnitude, electron density and net charge density for a case without photoionization and a background field of 15 kV/cm, at a time of 29 ns. The results show a typical single-filament postive streamer with enhancement of the electric field at its tip and a thin net positive charge layer surrounding the streamer channel. Figure 3 shows the time evolution of the streamer parameters plotted on the macroscopic parameter model chart. Here, the blue curve is a plot of streamer velocity (V) against tip electric field (E_T) and the red curve is a plot of streamer radius (R) against the channel electric field (E_{ch}). The time of the plotted points is indicated by the transparency of the markers. Earlier time points are more transparent and the markers become more opaque with increasing time. The correspondence of these two curves seems to be a good way to visualize how well the prediction of the quasi-steady 1.5D model (which the MPM model is based on) matches the results data. In this case, for the 2D streamer without photoionization, the overall shape of the curves seems to match well, as do the velocities, although there seems to be a larger discrepancy in the tip fields and radii. The MPM considers photoionization, whereas the 2D simulation does not in the case shown, so this particular example is not a good benchmark to assess the goodness of the MPM predictions.

Four cases were solved that included photoionization, with background electric fields of 15, 17.5, 20 and 23 kV/cm. The first two produced smooth single-filament streamers that looked similar to the results in Figure 2; however, the two simulations with higher fields showed numerical oscillations. Figure 4 shows result plots of electric field magnitude, electron density and net charge density for the case with photoionization and a background field of 20 kV/cm, at a time of 24 ns. The results show a streamer that appears to be close to branching, which can be most clearly seen in the middle plot of electron density. This case with photoionization and a lower background density seems generally more challenging to simulate - and it is possible that the cause of the oscillations may be due to inadequate mesh density and

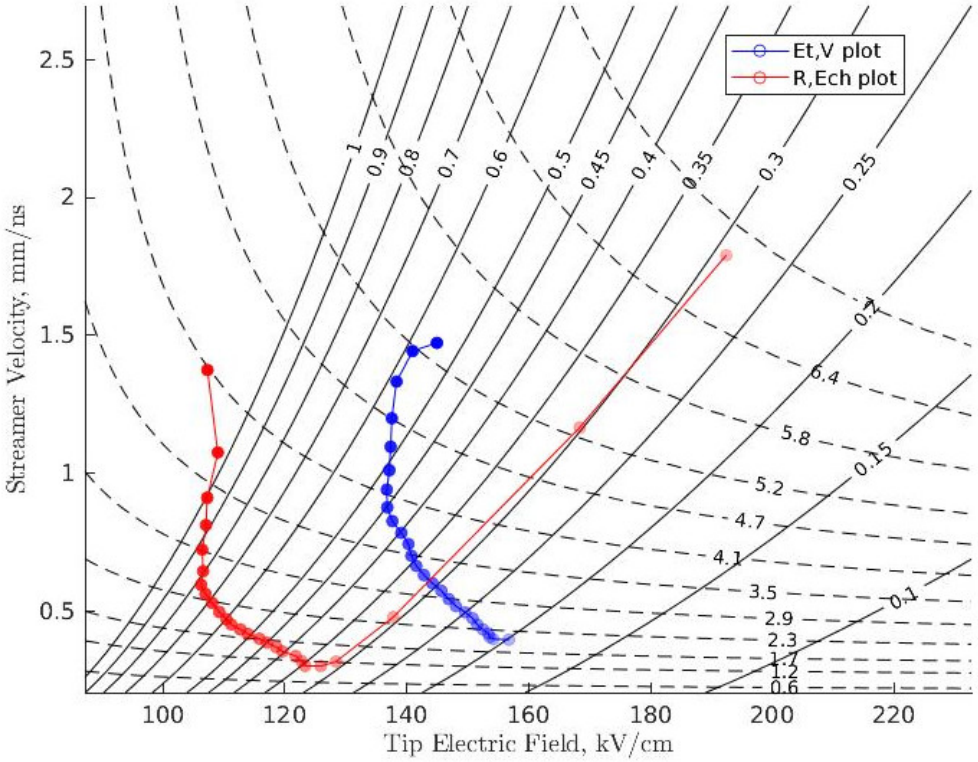

Fig. 3 Macroscopic parameter model overlaid with trajectories of 2D streamer without photoionization and background field of 15 kV/cm. Note that the MPM does consider photoionization whereas the 2D model does not in this case.

that refining the mesh may help to eliminate them. This issue is currently under investigation.

Figure 5 shows the macroscopic parameter map overlaid with trajectories for the streamer cases with photoionization and background electric fields of 15, 17.5, 20 and 23 kV/cm. The plots for 15 and 17.5 kV/cm are smooth; however, those for 20 and 23 kV/cm are considerably more noisy, which is likely due to the numerical instabilities mentioned above (tendency for branching). Despite the noise in the latter two plots, a general pattern seems evident: unlike the previous plot, here the tip electric fields seem to correspond quite well; however, there appears to be a larger discrepancy in the velocities. The red curve seems to increase in velocity more quickly than the blue curve, when comparing the same time points. There is also some strange behavior notable at later time points for figs 5c and 5d, which again may be a symptom of the numerical instabilities.

Figure 6 shows plots for all of the 2D HDG simulations run of the four key streamer parameters versus length: streamer radius, streamer velocity, maximum electric field and channel electric field. The 15 kV/cm case without photionization is shown as the dashed green line. Continuous lines correspond to cases that account for the full photoionization model. The radius and velocity both increase with length, which is consistent with the results of [22] for the cases shown with higher background electric fields. The cases with higher background fields seem to accelerate more quickly, which is as expected. The maximum electric fields seem to be similar for the cases with background fields up to 17.5 kV/cm. The cases with background fields of 20 and 23 kV/cm may have higher maximum electric fields; however, it is difficult to see with the noise. The channel field is higher for the cases with higher background fields, although it seems to increase with a similar gradient in all cases, once the streamer has developed. One interesting observation is that the channel field seems to show by far the largest discrepancy when comparing the 15 kV/cm cases with and without photoionization. Without photoionization, the channel field seems to lag significantly behind. The other three parameters seem to compare more closely.

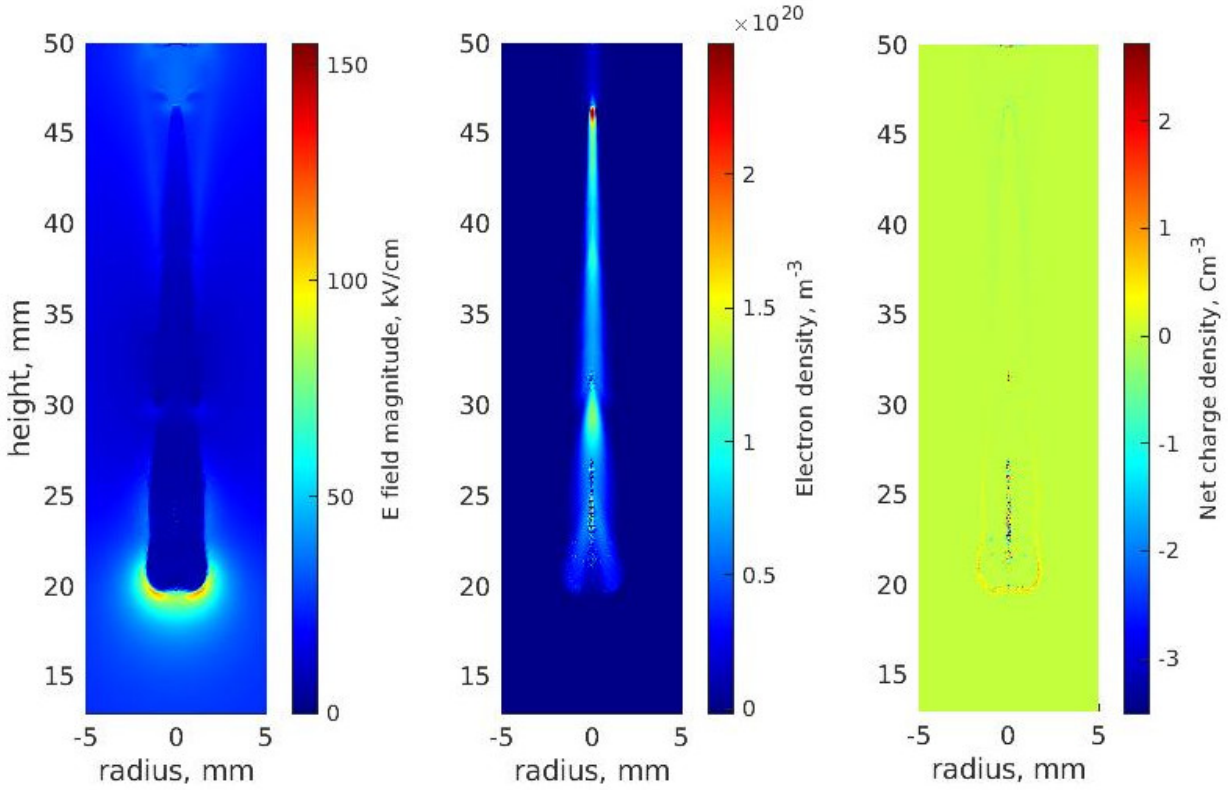

Fig. 4 Plots of electric field magnitude, electron density and net charge density for a simulation with photoionization and background field of 20 kV/cm, shown at 24 ns.

VI. Conclusions

The results presented here show that the Hybridizable Discontinuous Galerkin (HDG) numerical method developed by our group compares well with other state-of-the-art positive streamer codes [20] and can be used to further explore the physics of streamers. The results of the 2D HDG model also seem to be consistent with the results of [22], in that the streamer radius and velocity both increase with streamer length for uniform background fields exceeding 15 kV/cm. The authors of this work also found a similar pattern in that single-filament streamers are much harder to produce at background fields below 14-15 kV/cm.

When comparing the 2D models with and without photoionization, the largest difference was in the channel electric field. The streamer speed is less affected by the photoionization contribution.

Some interesting comparisons have been shown between the results of the 2D HDG streamer model and the quasi-steady 1.5D macroscopic parameter model from [11]. The general trends are well captured, even when plotting transient trajectories of streamers in the instantaneous quasi-steady approximation. The results of the MPM are better compared to the higher-fidelity simulation that includes photoinonization (since the MPM does account for a photoionization model). There does seem to be an over-prediction of the streamer speed when using the MPM to evaluate this parameter in terms of the streamer radius and channel field, particularly at the latter stages of development. This might provide some clues as to where the accuracy of the 1.5D steady-state model can be improved.

There is scope for further work in improving the 2D HDG model. For starters, the cases that include photoionization need to be addressed with a finer mesh, to see if that will reduce the numerical oscillations that were encountered. There may be some opportunities to use the results of the comparison with the 2D model to improve the 1.5D macroscopic model, which should be investigated further. It would also be very interesting to explore what happens to the accelerating streamers over longer time scales - it seems unlikely that they would accelerate indefinitely and must eventually reach some sort of steady-state condition. It would also be of interest to investigate streamers in lower background fields and to investigate tip-to-plate geometries, which would more closely approximate the conditions found in typical laboratory experiments.

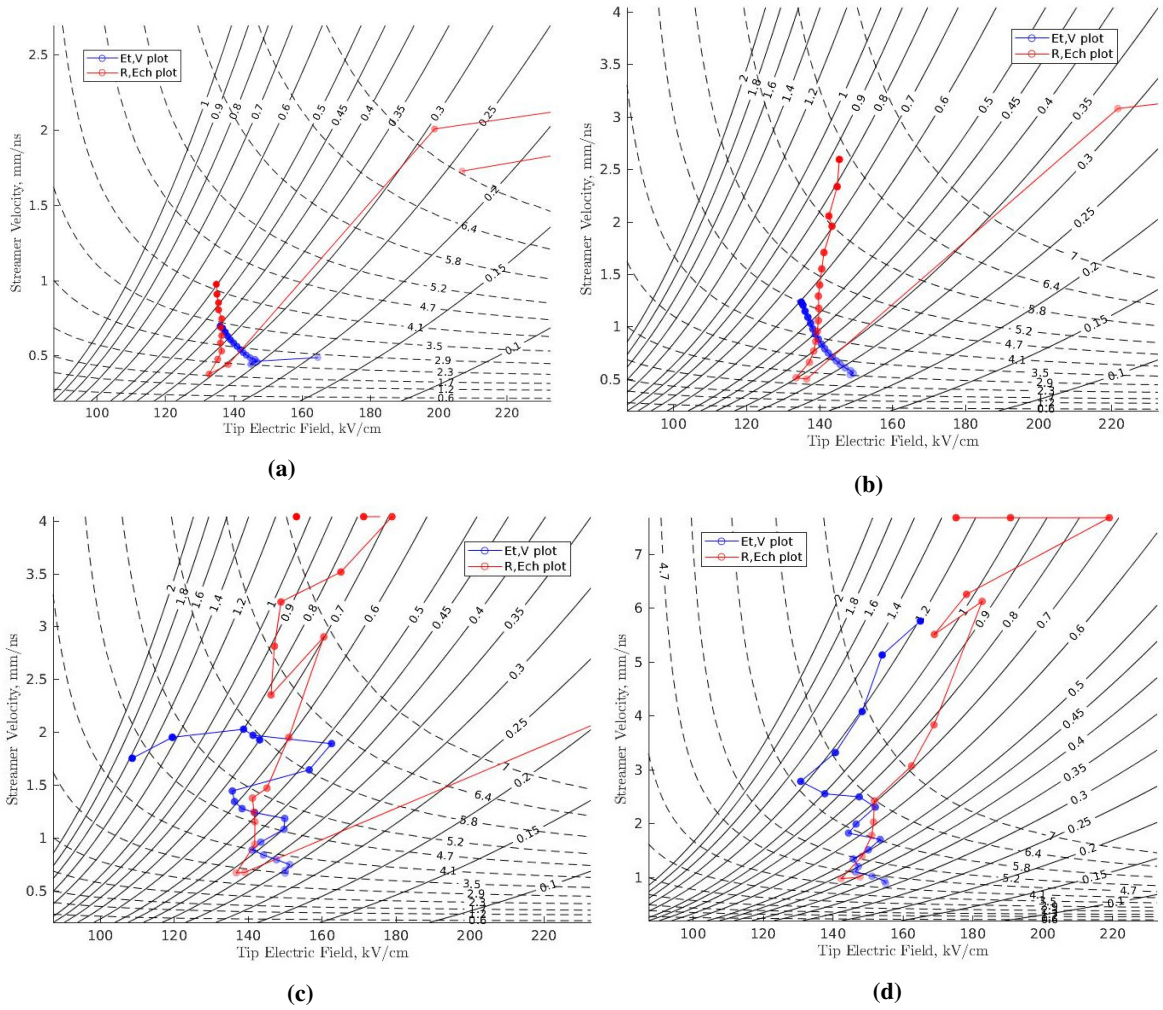

Fig. 5 Macroscopic parameter model overlaid with trajectories of 2D streamers simulated with photoionization and background fields of a) 15 kV/cm, b) 17.5 kV/cm, c) 20 kV/cm and d) 23 kV/cm. In this case, both the MPM and the 2D model have the photoionization models incorporated.

Acknowledgements

This work was partially supported by The Boeing Company through the Strategic Universities for Boeing Research and Technology Program. L. R. Strobel acknowledges partial support through a Linda and Richard Hardy fellowship (2020-2021) and a Mathworks fellowship (2021-2022). The authors thank Colin A. Pavan for help using the MPM code and Manuel Martinez-Sanchez for useful discussions.

References

[1] Kim, H.-H., "Nonthermal Plasma Processing for Air-Pollution Control: A Historical Review, Current Issues, and Future Prospects," *Plasma Processes and Polymers*, Vol. 1, No. 2, 2004, pp. 91–110. https://doi.org/10.1002/ppap.200400028.

[2] Fridman, G., Friedman, G., Gutsol, A., Shekhter, A. B., Vasilets, V. N., and Fridman, A., "Applied Plasma Medicine," *Plasma Processes and Polymers*, Vol. 5, No. 6, 2008, pp. 503–533. https://doi.org/10.1002/ppap.200700154.

[3] Starikovskiy, A., "Physics and chemistry of plasma-assisted combustion," *Philosophical Transactions of the Royal Society A: Mathematical, Physical and Engineering Sciences*, Vol. 373, No. 2048, 2015, p. 20150074. https://doi.org/10.1098/rsta.2015.0074.

[4] Pasko, V. P., "Red sprite discharges in the atmosphere at high altitude: the molecular physics and the similarity with laboratory

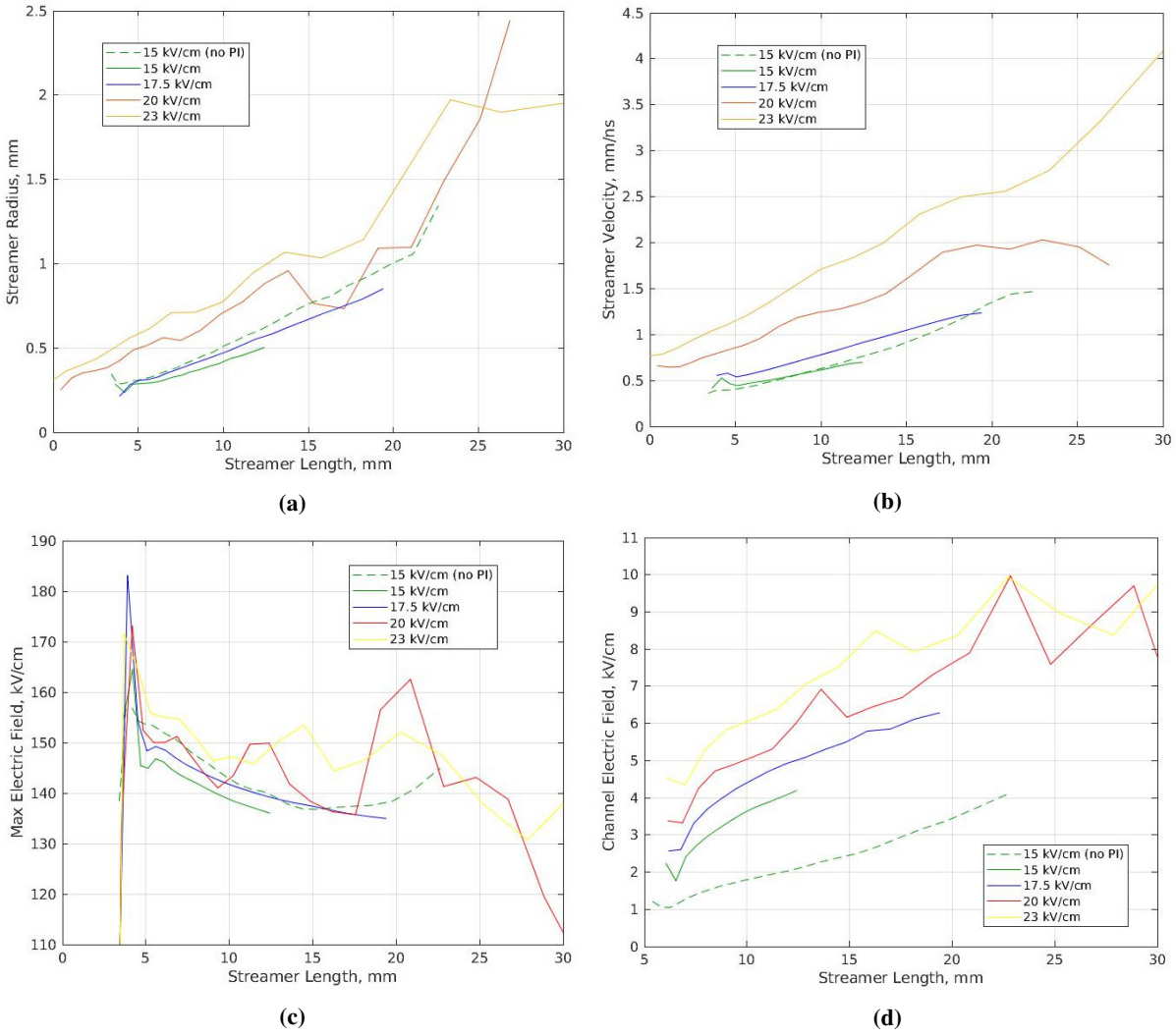

Fig. 6 Results of 2D high-fidelity model comparing background fields and the presence or not of a photoionization model. Plots of a) streamer radius versus length, b) streamer velocity versus length, c) maximum electric field and d) channel field for the streamer cases with (solid lines) and without (dashed line) photoionization.

discharges," *Plasma Sources Science and Technology*, Vol. 16, No. 1, 2007, pp. S13–S29. https://doi.org/10.1088/0963-0252/16/1/S02.

[5] van der Velde, O. A., Montanyà, J., López, J. A., and Cummer, S. A., "Gigantic jet discharges evolve stepwise through the middle atmosphere," *Nature Communications*, Vol. 10, No. 1, 2019, p. 4350. https://doi.org/10.1038/s41467-019-12261-y.

[6] Gallimberti, I., Bacchiega, G., Bondiou-Clergerie, A., and Lalande, P., "Fundamental processes in long air gap discharges," *Comptes Rendus Physique*, Vol. 3, No. 10, 2002, pp. 1335–1359. https://doi.org/10.1016/S1631-0705(02)01414-7.

[7] Luque, A., Ratushnaya, V., and Ebert, U., "Positive and negative streamers in ambient air: modelling evolution and velocities," *Journal of Physics D: Applied Physics*, Vol. 41, No. 23, 2008, p. 234005. https://doi.org/10.1088/0022-3727/41/23/234005.

[8] Papageorgiou, L., Metaxas, A. C., and Georghiou, G. E., "Three-dimensional numerical modelling of gas discharges at atmospheric pressure incorporating photoionization phenomena," *Journal of Physics D: Applied Physics*, Vol. 44, No. 4, 2011, p. 045203. https://doi.org/10.1088/0022-3727/44/4/045203.

[9] Teunissen, J., and Ebert, U., "Simulating streamer discharges in 3D with the parallel adaptive Afivo framework," *Journal of Physics D: Applied Physics*, Vol. 50, No. 47, 2017, p. 474001. https://doi.org/10.1088/1361-6463/aa8faf.

[10] Luque, A., and Ebert, U., "Growing discharge trees with self-consistent charge transport: the collective dynamics of streamers," *New Journal of Physics*, Vol. 16, No. 1, 2014, p. 013039. https://doi.org/10.1088/1367-2630/16/1/013039.

[11] Pavan, C., Martinez-Sanchez, M., and Guerra-Garcia, C., "Investigations of positive streamers as quasi-steady structures using reduced order models," *Plasma Sources Science and Technology*, Vol. 29, No. 9, 2020, p. 095004. https://doi.org/10.1088/1361-6595/aba863.

[12] Hagelaar, G. J. M., and Pitchford, L. C., "Solving the Boltzmann equation to obtain electron transport coefficients and rate coefficients for fluid models," *Plasma Sources Science and Technology*, Vol. 14, No. 4, 2005, pp. 722–733. https://doi.org/10.1088/0963-0252/14/4/011.

[13] Lawton, S. A., and Phelps, A. V., "Excitation of the b 1+g state of O2 by low energy electrons," *The Journal of Chemical Physics*, Vol. 69, No. 3, 1978, p. 1055. https://doi.org/10.1063/1.436700.

[14] "Phelps Database, retrieved June 2013," , ????. URL fr.lxcat.net.

[15] Phelps, A. V., and Pitchford, L. C., "Anisotropic scattering of electrons by N 2 and its effect on electron transport," *Physical Review A*, Vol. 31, No. 5, 1985, pp. 2932–2949. https://doi.org/10.1103/PhysRevA.31.2932.

[16] "Siglo Database, retrieved June 2013," , ????. URL fr.lxcat.net.

[17] Zhelezniak, M. B., Mnatsakanian, A. K., and Sizykh, S. V., "Photoionization of nitrogen and oxygen mixtures by radiation from a gas discharge," *High Temperature Science*, Vol. 20, No. 3, 1982, pp. 357–362.

[18] Bourdon, A., Pasko, V. P., Liu, N. Y., Célestin, S., Ségur, P., and Marode, E., "Efficient models for photoionization produced by non-thermal gas discharges in air based on radiative transfer and the Helmholtz equations," *Plasma Sources Science and Technology*, Vol. 16, No. 3, 2007, pp. 656–678. https://doi.org/10.1088/0963-0252/16/3/026.

[19] Nguyen, N., Peraire, J., and Cockburn, B., "An implicit high-order hybridizable discontinuous Galerkin method for nonlinear convection–diffusion equations," *Journal of Computational Physics*, Vol. 228, No. 23, 2009, pp. 8841–8855. https://doi.org/10.1016/j.jcp.2009.08.030.

[20] Bagheri, B., Teunissen, J., Ebert, U., Becker, M. M., Chen, S., Ducasse, O., Eichwald, O., Loffhagen, D., Luque, A., Mihailova, D., Plewa, J. M., van Dijk, J., and Yousfi, M., "Comparison of six simulation codes for positive streamers in air," *Plasma Sources Science and Technology*, Vol. 27, No. 9, 2018, p. 095002. https://doi.org/10.1088/1361-6595/aad768.

[21] Celestin, S., Bonaventura, Z., Zeghondy, B., Bourdon, A., and Ségur, P., "The use of the ghost fluid method for Poisson's equation to simulate streamer propagation in point-to-plane and point-to-point geometries," *Journal of Physics D: Applied Physics*, Vol. 42, No. 6, 2009, p. 065203. https://doi.org/10.1088/0022-3727/42/6/065203.

[22] Francisco, H., Teunissen, J., Bagheri, B., and Ebert, U., "Simulations of positive streamers in air in different electric fields: steady motion of solitary streamer heads and the stability field," *Plasma Sources Science and Technology*, 2021. https://doi.org/10.1088/1361-6595/ac2f76.